Title

Rewiring a Rab regulatory network reveals a possible inhibitory role for the vesicle tether, Uso1

Journal

Proceedings of the National Academy of Sciences of the United States of America, 114(41)

ISSN

0027-8424

Authors

Yuan, Hua
Davis, Saralin
Ferro-Novick, Susan
et al.

Publication Date

2017-10-10

DOI

10.1073/pnas.1708394114

Peer reviewed

Rewiring a Rab regulatory network reveals a possible inhibitory role for the vesicle tether, Uso1

Hua Yuan[a], Saralin Davis[a], Susan Ferro-Novick[a], and Peter Novick[a,1]

[a]Department of Cellular and Molecular Medicine, University of California, San Diego, La Jolla, CA 92093

Contributed by Peter Novick, September 1, 2017 (sent for review May 22, 2017; reviewed by Charles Barlowe and Suzanne R. Pfeffer)

Ypt1 and Sec4 are essential Rab GTPases that control the early and late stages of the yeast secretory pathway, respectively. A chimera consisting of Ypt1 with the switch I domain of Sec4, Ypt1-SW1^{Sec4}, is efficiently activated in vitro by the Sec4 exchange factor, Sec2. This should lead to its ectopic activation in vivo and thereby disrupt membrane traffic. Nonetheless early studies found that yeast expressing Ypt1-SW1^{Sec4} as the sole copy of *YPT1* exhibit no growth defect. To resolve this conundrum, we have analyzed yeast expressing various levels of Ypt1-SW1^{Sec4}. We show that even normal expression of Ypt1-SW1^{Sec4} leads to kinetic transport defects at a late stage of the pathway, with secretory vesicles accumulating near exocytic sites. Higher levels are toxic. Toxicity is suppressed by truncation of Uso1, a vesicle tether required for endoplasmic reticulum–Golgi traffic. The globular head of Uso1 binds to Ypt1 and its coiled-coil tail binds to the Golgi-associated SNARE, Sed5. We propose that when Uso1 is inappropriately recruited to secretory vesicles by Ypt1-SW1^{Sec4}, the extended coiled-coil tail blocks docking to the plasma membrane. This putative inhibitory function could serve to increase the fidelity of vesicle docking.

membrane traffic | Rab GTPase | vesicle tether

Rab GTPases are master regulators of vesicular transport, each typically controlling a particular stage of membrane traffic. Rabs are activated by guanine nucleotide exchange factors (GEFs) that catalyze the exchange of GDP for GTP and inactivated by GTPase-activating proteins (GAPs) that stimulate the slow intrinsic rate of GTP hydrolysis (1). Since GDP- but not GTP-bound Rabs are extracted from membranes by GDP dissociation inhibitor (2), the localization of a GEF plays a key role in defining the localization of its substrate Rab (3–5). Once in their GTP-bound state, each Rab recruits a distinct set of effectors, such as, motors that drive vesicle movement, tethers that direct vesicle-target recognition, and regulators of the SNAREs that catalyze fusion (6). By defining when and where each Rab enters and exits its GTP-bound form, GEFs and GAPs help to establish the functional identity and directionality of vesicular carriers (1).

While each Rab displays a distinctive pattern of localization, adjacent Rabs are often functionally linked to each other through their regulators (1). Here we focus on the yeast secretory pathway in which Ypt1, a Rab1 homolog, controls transport from the endoplasmic reticulum (ER) to the Golgi (7, 8); Ypt31 and Ypt32, redundant Rab11 homologs, control exit from the Golgi (9, 10), and Sec4, a Rab 8 homolog, promotes delivery of Golgi-derived secretory vesicles to sites of exocytosis (11). Sec2 is an efficient and specific GEF for Sec4 and, like Sec4, it is concentrated on the surface of Golgi-derived secretory vesicles (4, 12). The association of Sec2 with those vesicles relies upon its interaction with the GTP-bound forms of either of the upstream Rabs, Ypt31 and Ypt32 (13, 14). This relationship constitutes a Rab GEF cascade in which one Rab recruits the GEF that activates the next Rab. A directly analogous relationship has been established for the mammalian homologs in which Rab11-GTP recruits Rabin 8, a Sec2 homolog, which then activates Rab8 (15). Additional Rab GEF cascades have been identified on other trafficking pathways (16–21). Several Rab GAPs have been implicated in opposing GAP cascades (22–25). On the yeast secretory pathway Gyp1, a GAP that inactivates Ypt1 (26), is recruited to the late Golgi by binding to Ypt32-GTP, thus limiting the extent of overlap between the Ypt1 and Ypt32 domains (25). GEF and GAP cascades, working together in a countercurrent fashion, could lead to a series of abrupt transitions from one Rab to the next as membrane flows along a pathway (1). In principle, by coupling localization domains that recognize the active form of one Rab to catalytic domains that either activate a downstream Rab or inactivate an upstream Rab, a defined program of Rab transitions could be specified that would lead to ordered changes in membrane identity (1).

Here we probe this model by exploiting a fascinating allele of *YPT1* to rewire the Rab regulatory circuit on the yeast secretory pathway. In early studies, various domains of Ypt1 and Sec4 were swapped and the resulting chimeras analyzed in vivo to establish the structural basis of Rab specificity (27, 28). One such chimera was originally named Ypt1-EF^{Sec4}, to denote the replacement of the putative effector domain of Ypt1 with that of Sec4 (27), but subsequently renamed Ypt1-SW1^{Sec4} to describe more accurately the structural element (switch 1) that had been swapped (29). When expressed at normal levels from the endogenous promoter, this chimera was found to function as the sole copy of the essential *YPT1* gene without any significant growth defect or inhibition in the export of the cell wall enzyme invertase (27). This result implies that Ypt1-SW1^{Sec4} must be able to interact productively with all of the essential Ypt1 regulators and effectors.

The Ypt1-SW1^{Sec4} chimera resurfaced in the context of a crystallographic study of Sec2 bound to its substrate, Sec4 (29). The structure indicated that the main contacts with Sec2 involved the switch 1 and switch 2 domains of Sec4. As the switch 2 domain of Ypt1 is nearly identical to that of Sec4, this led to the prediction that replacing the switch 1 domain of Ypt1 with that of Sec4 would allow the chimera to interact with Sec2. The prediction held up:

Significance

Members of the Rab family act as molecular switches to control distinct stages of vesicular traffic into and out of a eukaryotic cell. Many Rabs are linked to the adjacent Rab by their regulators, generating circuits that direct transport along the pathway. We have rewired one such regulatory circuit by exploiting a chimeric Rab that acts early on the pathway but can be activated by a regulator that is situated late on the pathway. Expression of this chimeric Rab leads to a block late on the pathway. Our findings confirm the importance of Rabs in establishing membrane identity.

Author contributions: H.Y., S.D., S.F.-N., and P.N. designed research; H.Y. and S.D. performed research; H.Y., S.D., and S.F.-N. contributed new reagents/analytic tools; H.Y., S.D., S.F.-N., and P.N. analyzed data; and H.Y. and P.N. wrote the paper.

Reviewers: C.B., Dartmouth College; and S.R.P., Stanford University School of Medicine.

The authors declare no conflict of interest.

[1]To whom correspondence should be addressed. Email: pnovick@ucsd.edu.

This article contains supporting information online at www.pnas.org/lookup/suppl/doi:10.1073/pnas.1708394114/-/DCSupplemental.

although Sec2 has no activity with Ypt1, it efficiently activates Ypt1-SW1^{Sec4} in vitro (29). Taken together, these two studies present a conundrum: Ypt1-SW1^{Sec4} fulfills all of the essential Ypt1 roles early on the secretory pathway, yet it can be activated in vitro by a GEF that resides at the end of the pathway. If Rabs define the identity of the membrane with which they are associated, then Ypt1-SW1^{Sec4} expression should trigger havoc in the cell by leading to Ypt1 activity on the wrong part of the secretory pathway. Nonetheless, phenotypic analysis suggested that this was not the case (27). Here we consider three possible resolutions to this conundrum: (*i*) Sec2 does not actually activate Ypt1-SW1^{Sec4} in vivo, despite the exchange activity observed in vitro; (*ii*) Ypt1-SW1^{Sec4} expression is not as benign as it first appeared; or (*iii*) the proposal that Rabs define membrane identity is seriously flawed. Our studies not only confirm the importance of Rabs to membrane identity, they have also revealed a possible inhibitory function for the long, coiled-coil vesicle tether Uso1. This tether normally acts in response to Ypt1-GTP to form the initial link between ER-derived vesicles and the Golgi apparatus (30). We find that, when inappropriately recruited to post-Golgi secretory vesicles by Ypt1-SW1^{Sec4}, Uso1 acts to inhibit their fusion with the plasma membrane.

Results

To determine if Sec2 can activate Ypt1-SW1^{Sec4} in vivo as it does in vitro (29), we conducted both genetic tests and localization studies. Ypt1 is normally activated by the TRAPP complexes and the Bet3 subunit is critical for this GEF activity (31). If Ypt1-SW1^{Sec4} can be activated by Sec2p in vivo, its expression might alleviate the growth defect of a *bet3* mutant. Fig. 1*A* shows that *bet3-1* cells fail to grow at temperatures higher than 30 °C. Expression of Ypt1 from the *GPD* promoter allows somewhat stronger growth at 30 °C, but not at 33 °C, while expression of Ypt1-SW1^{Sec4} confers strong growth at 33 °C. Immunoblot analysis indicates similar levels of expression of Ypt1 and Ypt1-SW1^{Sec4} from the GPD promoter (Fig. S1*A*). This result is consistent with the hypothesis that Sec2 activates Ypt1-SW1^{Sec4} in vivo.

The localization of a GEF plays a major role in determining the localization of its substrate Rab (3, 5). Sec2 is associated primarily with secretory vesicles (12). These vesicles are delivered to sites of polarized cell surface growth, such as the tips of small buds or the necks of large budded cells where, after a brief delay, they fuse with the plasma membrane (32, 33). Sec2, as well as its substrate Rab, Sec4, are therefore highly concentrated at these polarized growth sites (12). If Sec2 activates Ypt1-SW1^{Sec4} in vivo, we would expect the localization of Ypt1-SW1^{Sec4} to at least partially overlap with that of Sec2. We expressed mCherry-tagged Ypt1 (mCh-Ypt1) or Ypt1-SW1^{Sec4} (mCh-Ypt1-SW1^{Sec4}) in wild-type cells. mCh-Ypt1 is associated with Golgi cisternae, which appear as dispersed puncta with less than 4% of the cells exhibiting a concentration at sites of polarized surface growth (Fig. 1 *C* and *D*). In contrast, about 80% of the cells expressing mCh-Ypt1-SW1^{Sec4} exhibit a prominent concentration at either the tip of a small bud or the neck of a large-budded cell, mimicking the distribution of Sec2 or its substrate, Sec4 (Fig. 1 *C* and *D*). Partial colocalization with Sec2-GFP was observed, further supporting the hypothesis that Sec2 activates Ypt1-SW1^{Sec4} in vivo (Fig. 1 *E* and *F*). The ability of Ypt1-SW1^{Sec4} to suppress *bet3-1* more efficiently than Ypt1 (Fig. 1*A*) likely reflects the existence of a significant soluble pool of Sec2 (12) that could lead to the activation of a fraction of Ypt1-SW1^{Sec4} on the early secretory pathway, where it could fulfill the essential roles of Ypt1.

In a prior study we found that Ypt1-SW1^{Sec4} expressed from the endogenous *YPT1* promoter can function as the sole copy of *YPT1* with no obvious growth defect (27). However, the mislocalization of mCh-Ypt1-SW1^{Sec4} led us to examine the effects of varying levels of Ypt1-SW1^{Sec4} expression on growth and

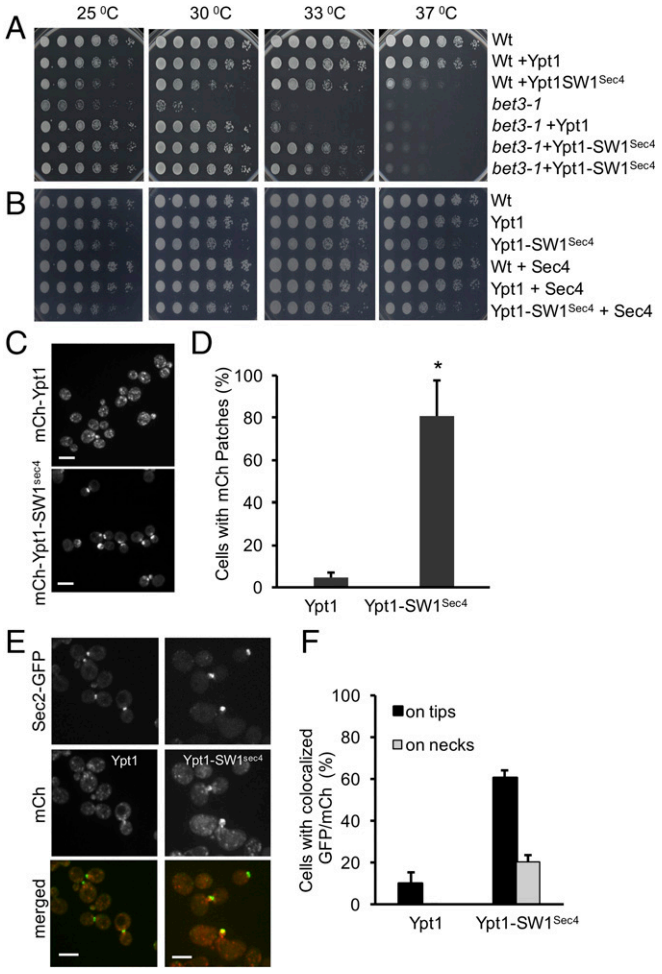

Fig. 1. (*A*) Expression of Ypt1-SW1^{Sec4} suppresses *bet3-1*. Wild-type (NY834) (top three rows) or *bet3-1* (SFNY380) cells (bottom four rows) were transformed with plasmids expressing either Ypt1 (yielding NY3188 and NY3190) or Ypt1-SW1^{Sec4} (yielding NY3189 and NY3191) from the *GPD1* promoter on a CEN vector and then grown in SC-URA medium. The parental strains and transformants were spotted in serial dilutions onto plates and incubated at the indicated temperatures for 3 d. Ypt1-SW1^{Sec4}, but not Ypt1, suppresses the *bet3-1* growth defect at 33 °C. Inhibition of wild-type cell growth is seen upon Ypt1-SW1^{Sec4} expression from this promoter at 37 °C. (*B*) Overexpression of Sec4 does not suppress the growth defect resulting from expression of Ypt1-SW1^{Sec4}. Wild-type expressing Ypt1 or Ypt1-SW1^{Sec4} from the *GPD1* promoter on a CEN vector (NY834, NY3188, NY3189) were transformed with a 2-μ plasmid expressing Sec4 (yielding NY3299 NY3300, NY3301). The growth test was carried out using the same conditions as in *A*. (*C*–*F*) Ypt1-SW1^{Sec4} localizes to polarized sites and colocalizes with Sec2p in yeast cells. (*C*) Yeast cells expressing mCh-Ypt1 (NY3192) or mCh-Ypt1-SW1^{Sec4} (NY3193) were grown to early log phase in SC-LEU medium at 25 °C. Cells were harvested and imaged by confocal fluorescence microscope. (Scale bar, 5 μm.) (*D*) The percentage of cells with polarized mCherry signal was quantified. Error bars represent SD from four independent experiments. At least 200 cells were scored for each strain. *$P < 0.0005$ Student's *t* test. (*E*) Cells coexpressing Sec2-GFP and mCh-Ypt1 (NY3194) or mCh-Ypt1-SW1^{Sec4} (NY3195) were grown to early log phase in synthetic medium at 25 °C. Next, 500 μL of cells were collected and images were captured using a confocal fluorescence microscope. (Scale bars, 5 μm.) (*F*) Quantification of colocalization of Sec2-GFP and mCh-Ypt1 or mCh-Ypt1-SW1^{Sec4}.

membrane traffic. When we introduced a plasmid expressing Ypt1-SW1^{Sec4} from the *GPD* promoter into wild-type cells, the transformants grew well at intermediate temperatures, but exhibited slow growth at 37 °C (Fig. 1*B*). We therefore constructed a plasmid expressing Ypt1-SW1^{Sec4} from the strong,

inducible *GAL1* promoter. Transformants grew well on medium containing glucose, a repressing carbon source, but failed to grow on inducing galactose medium (Fig. 2*A*). Control strains expressing Ypt1 under *GAL* regulation grew well on both media (Fig. 2*A*). Therefore, *YPT1-SW1*^{Sec4} is a dose-dependent, dominant-negative allele. Western blots indicate that the *GPD* promoter led to approximately twofold overexpression of Ypt1-SW1^{Sec4}, while the *GAL* promoter led to ninefold overexpression (Fig. S1*B*).

Cells expressing Ypt1-SW1^{Sec4} from the *GAL1* promoter began to slow in growth rate 7 h after a shift from raffinose medium to galactose medium (Fig. S2). We therefore examined secretory pathway function after 5 h of induction. The cell wall glucanase Bgl2 is exported efficiently by wild-type cells with only a minor internal pool of transport intermediates (Fig. 2 *B* and *D*). A temperature-sensitive *sec6-4* strain, used as a control, accumulated a large internal pool and a reduced external pool of Bgl2 at its restrictive temperature, 37 °C. Cells expressing Ypt1-SW1^{Sec4} from the *GAL* promoter exhibited a large internal pool at both 25 °C and 37 °C, indicating a severe secretory defect (Fig. 2 *B* and *D*).

To determine the site of the block along the secretory pathway, we examined cells by thin section electron microscopy (EM). Cells expressing Ypt1 from the *GAL* promoter exhibited a normal morphology (Fig. 3*A*), while most cells expressing Ypt1-SW1^{Sec4} accumulated a large number of 100-nm vesicles (Fig. 3*B*). Some cells also contained several cup-shaped structures that likely represent aberrant forms of Golgi cisternae (34). These phenotypes are consistent with a defect late on the secretory pathway.

The exocytic v-SNARE, Snc1, is delivered in secretory vesicles to the plasma membrane, then internalized into endosomes and the *trans*-Golgi network, from which it enters a new round of vesicles in an ongoing cycle (35). At steady-state, GFP-Snc1 is predominantly at the plasma membrane with only a few internal puncta, representing endosomes and the *trans*-Golgi network (Fig. 4*A*). Following induction of Ypt1-SW1^{Sec4}, prominent GFP-Snc1 concentrations were observed at bud tips and bud necks, internal to the cell surface, indicating a slowing of the traffic cycle at a point after vesicles have been delivered to exocytic sites, but before their fusion with the plasma membrane.

We also examined the secretory pathway function in cells expressing Ypt1-SW1^{Sec4} at normal levels as the sole copy of Ypt1. Although these cells grow well, the internal pool of Bgl2 was increased several-fold with respect to that of wild-type cells, indicating a modest secretory defect (Fig. 2 *C* and *E*). Thin-section EM revealed the accumulation of 100-nm secretory vesicles (Fig. 3 *D*, *F*, and *G*). In cells that had been sectioned through the mother–bud axis, the vesicles were highly concentrated toward the tips of the bud. No accumulation of cup-shaped, Golgi-related structures was evident, unlike cells expressing Ypt1-SW1^{Sec4} from the *GAL* promoter. GFP-Snc1 was concentrated at tips of small buds and near the necks of large budded cells expressing Ypt1-SW1^{sec4} from the endogenous promoter (Fig. 4 *B* and *C*). In total, the results indicate that, even at normal levels of expression, when the growth rate is not significantly affected, Ypt1-SW1^{Sec4} leads to a kinetic block of the secretory pathway at a point after secretory vesicles have been delivered to exocytic sites, but before their fusion with the plasma membrane. The Golgi-related structures that appear in some cells expressing Ypt1-SW1^{Sec4} from the *GAL* promoter could result from the strong, protracted block in the pathway that in time leads to a back-up at an earlier stage, as has been observed in various late-blocked *sec* mutants (36).

In a prior study we did not observe a significant defect in the secretion of the cell wall enzyme invertase in cells expressing Ypt1-SW1^{Sec4} from the *YPT1* promoter (27). We have confirmed these observations, finding a small but not statistically significant reduction in the efficiency of invertase secretion (Fig. S3*A*). Invertase is delivered to the cell surface by vesicles of a higher

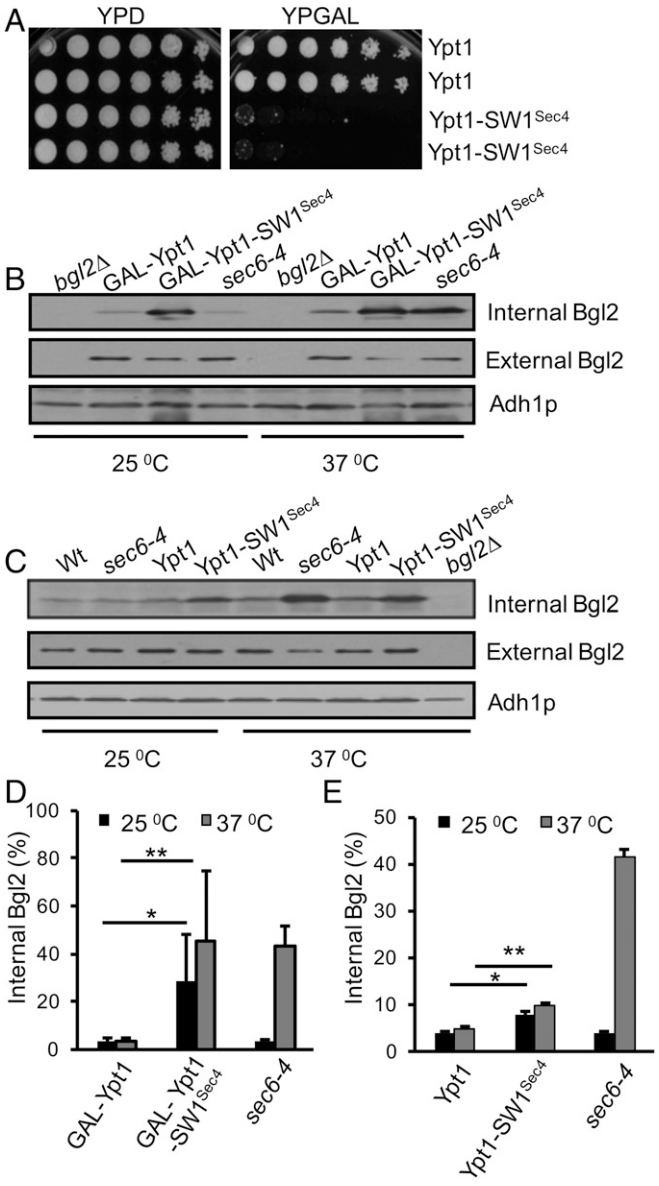

Fig. 2. Overexpression of Ypt1-SW1^{Sec4} is toxic and inhibits Bgl2 secretion. (*A*) Yeast cells harboring GALpYpt1(NY3196) or GALpYpt1-SW1^{Sec4} (NY3197) expression constructs were grown in YPD overnight. Next, 1.25 OD_{600} units of cells from each strain were harvested for a growth test on YPD medium or washed once in sterile water and spotted onto a YPGAL plate. Plates were incubated at 25 °C for 2 d. (*B*) Overexpression of Ypt1-SW1^{Sec4} blocks secretion of the Bgl2 glucanase. GALpYpt1 (NY3196), GALpYpt1-SW1^{Sec4} (NY3197), and the control strains *sec6-4* (NY17) and *bgl2*Δ (NY3072), were grown at 25 °C in YP +2% raffinose medium overnight to early log phase, shifted to YP +2% galactose medium for 4 h at 25 °C, and then an additional 90 min at either 25 °C or 37 °C, as indicated. Internal and external fractions were prepared as described in *Materials and Methods*. Ten-fold more of the internal fraction was loaded relative to the external fraction. Bgl2 was visualized by Western blotting using anti-Bgl2 rabbit polyclonal antibody and Adh1 was visualized as a loading control. (*C*) Bgl2 secretion is also inhibited in strains expressing Ypt1-SW1^{Sec4} from the endogenous promoter, as the sole copy of *YPT1*. Wild-type (NY1210), *YPT1* (NY1048), *YPT1-SW1*^{Sec4} (NY1052), *sec6-4* (NY17), and *bgl2*Δ (NY3072) strains were grown in YPD medium overnight. Each culture was divided into two aliquots and grown for an additional 90 min at 25 °C or 37 °C, as indicated. Bgl2 and Adh1 were detected as described above. (*D*) Quantitation of internal Bgl2 in cells of *B*. Error bars represent SD, $n = 5$. $^{*}P < 0.0228$, $^{**}P < 0.0310$. (*E*) Quantification of internal Bgl2 in cells of *C*. Error bars represent SD, $n = 5$. $^{*}P < 0.0008$, $^{**}P < 0.0013$.

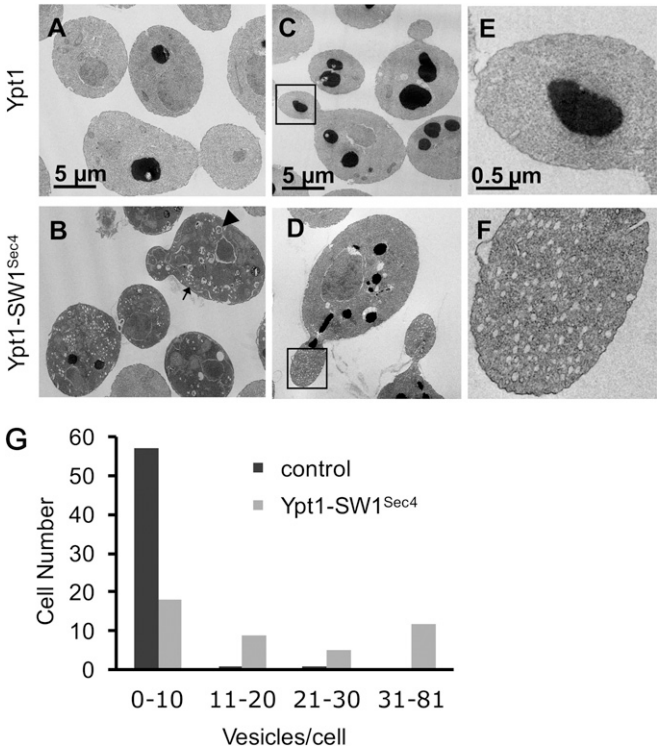

Fig. 3. Thin-section EM indicates that Ypt1-SW1^{Sec4} expression leads to secretory vesicle accumulation. (*A*) Cells expressing GALpYpt1 (NY3196) or (*B*) GALpYpt1-SW1^{Sec4} (NY3197) were grown in YP +2% galactose for 7 h and prepared for EM, as described in *Materials and Methods*. Arrow shows a vesicle. Arrowhead shows a Golgi-related structure. (*C–F*) Cells expressing Ypt1 (NY1048) (*C* and *E*) or Ypt1-SW1^{Sec4} (NY1052) (*D* and *F*) at normal levels from the endogenous promoter as the sole copy of *YPT1*. *E* and *F* show expanded boxed regions from *C* and *D*, respectively. Scale bars as indicated. (*G*) Quantitation of secretory vesicles. The number of vesicles per cell was scored from EM images. Sixty cells were analyzed for wild-type (NY1048) and 44 cells for Ypt1SW1^{Sec4} expressed from the endogenous promoter (NY1052).

buoyant density than those used for export of Bgl2, and the invertase vesicles (37) are thought to bud from endosomes rather than the Golgi (38). To determine if the apparent insensitivity of invertase secretion to Ypt1-SW1^{Sec4} expression reflects a fundamental mechanistic difference, we examined the efficiency of invertase secretion in cells expressing Ypt1-SW1^{Sec4} from the stronger *GPD1* promoter. A somewhat larger, statistically significant defect was observed (Fig. S3*B*), indicating that secretion of invertase, like Bgl2, is subject to inhibition by Ypt1-SW1^{Sec4}.

The formation of secretory vesicles from the Golgi requires Ypt32 or its paralog Ypt31 (9, 10) and these Rabs are incorporated into the newly formed vesicles. However, as vesicles mature, Ypt31/32 is normally lost and Sec4 is recruited (33). We examined the localization of Ypt32 and Sec4 in strains expressing Ypt1-SW1^{Sec4}. In cells expressing Ypt1, GFP-Ypt32 exhibits only a minor accumulation at sites of polarized cell surface growth, with most of the protein localized to puncta distributed throughout the cytosol (Fig. 5 *A* and *C*). In cells expressing Ypt1-SW1^{Sec4}, GFP-Ypt32 exhibits very prominent concentrations in small buds and the necks of large budded cells (Fig. 5 *A* and *C*). GFP-Sec4 is also concentrated at bud tips and necks in cells expressing either Ypt1 or Ypt1-SW1^{Sec4} (Fig. 5 *B* and *D*). Thus, the vesicles accumulating as a result of Ypt1-SW1^{Sec4} expression appear to carry both Ypt32 and Sec4, although it is also possible that two vesicle populations accumulate at sites of polarized growth, one carrying Ypt32, the other carrying Sec4.

Ypt1-SW1^{Sec4} expression might be expected to drive the ectopic recruitment of Ypt1 effectors to secretory vesicles. We examined the localization of three different components of the secretory machinery that have each been implicated as Ypt1 effectors: Cog3, Sec7, and Uso1 (30, 39, 40). All of these components are normally associated with Golgi cisternae and therefore appear in wild-type cells as punctate structures, with little evident polarization toward bud tips or necks. In the cases of Cog3 and Sec7, there was little difference in localization between cells expressing Ypt1 or Ypt1-SW1^{Sec4} (Fig. 6 *A*, *B*, and *D*). In the case of Uso1, however, a striking change was seen. A shift of Uso1-3xGFP to bud tips and necks was observed in a large fraction of cells expressing Ypt1-SW1^{Sec4} (Fig. 6 *C* and *D*).

We have used suppressor analysis to address the mechanism of inhibition of vesicle traffic by Ypt1-SW1^{Sec4}. Since Sec2 can recognize and activate Ypt1-SW1^{Sec4}, it is plausible that Ypt1-SW1^{Sec4} competes against the normal substrate, Sec4, for a limiting pool of Sec2. This would reduce the level of Sec4-GTP and therefore inhibit the secretory pathway at a late stage. Another possible mechanism of inhibition would be interference by

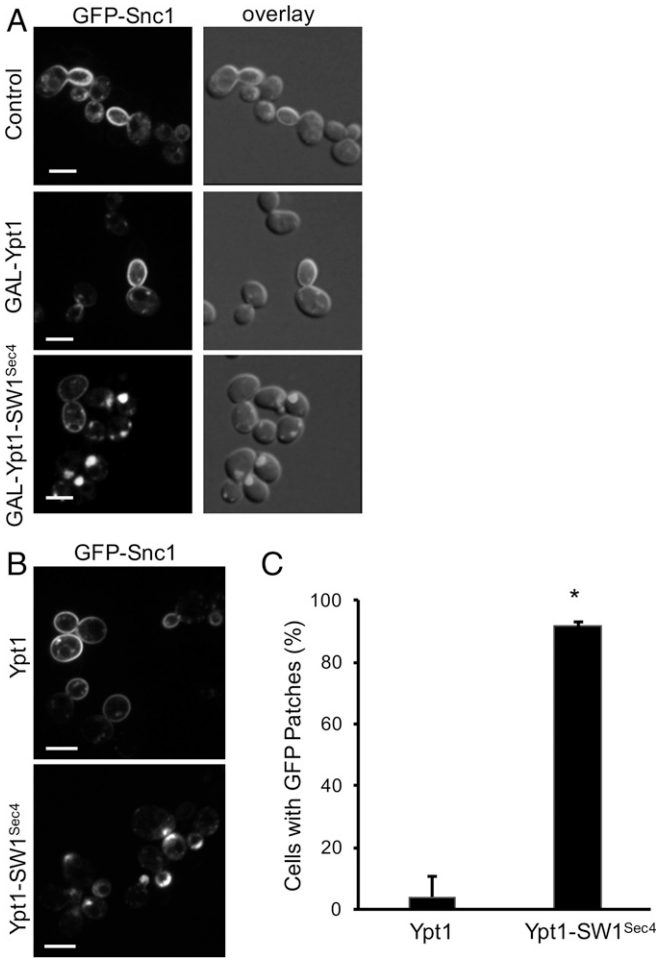

Fig. 4. Expression of Ypt1-SW1^{Sec4} leads to intracellular GFP-Snc1 accumulation. (*A*) Wild-type (NY1210), GALpYpt1 (NY3204), and GALpYpt1-SW1^{sec4} (NY3205) strains harboring a CEN plasmid expressing GFP-Snc1 (SFNB1223) were grown in SC +2% raffinose medium to early log phase, and then shifted to medium containing 2% galactose for 4 h at 25 °C. Images were captured by confocal microscope. (*B*) Strains expressing Ypt1(NY3198) or Ypt1-SW1^{sec4} (NY3199) as the sole copy of Ypt1 from the endogenous promoter were transformed with a CEN plasmid expressing GFP-Snc1 (SFNB1223). Localization of GFP-Snc1 was examined. (Scale bars, 5 um.) (*C*) Quantification of cells with GFP patches from *B*. Error bars represent SD; $n = 3$, $^*P < 0.000012$.

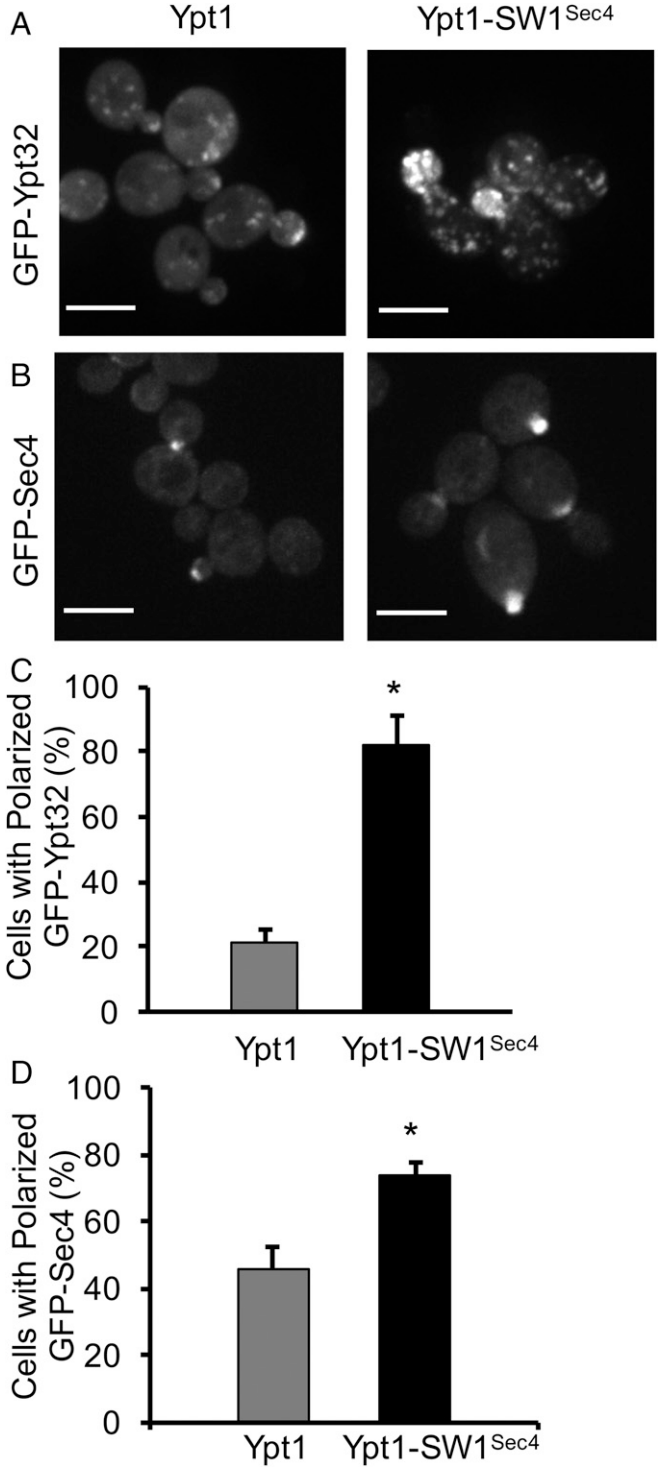

Fig. 5. Localization of GFP-Ypt32p and GFP-Sec4p in cells expressing Ypt1 or Ypt1-SW1^{Sec4} as the sole copy of Ypt1 from the endogenous promoter. (*A*) Images of GFP-Ypt32 in Ypt1 cells (NY3202) or Ypt1-SW1^{Sec4} cells (NY3203). (*B*) Images of GFP-Sec4 in strains expressing Ypt1 (NY3200) or Ypt1-SW1^{Sec4} (NY3201). Cells were grown in selection medium to log phase at 25 °C. Next, 500 μL of the culture was collected and imaged by confocal microscope. (Scale bar, 5 μm.) (*C*) Quantification of the percentage of cells exhibiting a polarized distribution of GFP-Ypt32 or (*D*) GFP-Sec4. Error bars represent SD; $n = 3$, $^*P < 0.001$ for Ypt32 (*C*) and $P < 0.005$ for Sec4 (*D*).

Ypt1-SW1^{Sec4} in the interaction of Sec4-GTP with one of its effectors. We overexpressed either Sec2 or Sec4, from high copy-number plasmids, in cells expressing Ypt1-SW1^{Sec4} from the *GAL* promoter. No restoration of growth on galactose medium was observed in these strains (Fig. 7*A*). We also overexpressed Sec4 in cells expressing Ypt1-SW1^{Sec4} from the weaker GPD promoter. The growth defect observed at 37 °C was unaffected by increased Sec4 expression (Fig. 1*B*). Therefore, it appears unlikely that competition against Sec4 represents the mechanism of vesicle traffic inhibition by Ypt1-SW1^{Sec4}. Furthermore, expression of Ypt1-SW1^{Sec4} from the *GAL* promoter has no effect on the expression level of either Sec4 or its effector Sec15 (Fig. S1*C*).

Another plausible mechanism involves the ectopic recruitment of Ypt1 effectors to the secretory vesicle membrane by Ypt1-SW1^{Sec4}. The inappropriate presence of one or more Ypt1 effectors on the vesicle surface might inhibit its ability to dock and fuse with the plasma membrane. Since Uso1 redistributes to exocytic sites in response to Ypt1-SW1^{Sec4} expression, while Cog3 and Sec7 do not, we tested the ability of two loss-of-function alleles of *uso1* to suppress the galactose-dependent toxicity of GALpYpt1-SW1^{Sec4} expression. The *uso1-1* mutation truncates the 1,790-residue-long protein at amino acid 950. This results in temperature-sensitive defects in growth and secretion (41). However, at permissive temperatures the *uso1-1* strain was significantly resistant to the galactose-dependent toxicity of GALp Ypt1-SW1^{Sec4} expression (Fig. 7*B*). The *uso1-10* allele truncates the protein at amino acid

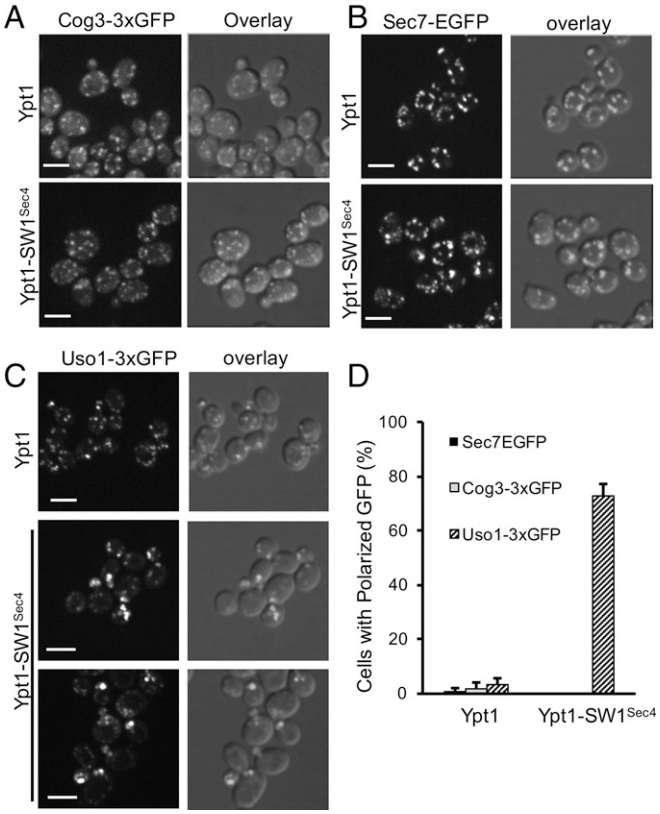

Fig. 6. GALpYpt1-SW1^{Sec4} expression affects a subset of Ypt1 effectors. Cells were grown in selection medium containing 2% galactose for 5 h at 25 °C. GFP fusion proteins were visualized by confocal fluorescence microscope. The overlay panels show a merge of the fluorescence image and a DIC image. (*A*) Yeast cells coexpressed Cog3-3xGFP (pNB1620) with GALpYpt1 (NY3206) or GALpYpt1SW1^{Sec4} (NY3207). (*B*) Yeast cells coexpressed Sec7-EGFP (SFNB797) with GALpYpt1 (NY3208) or GALpYpt1SW1^{Sec4} (NY3209). (*C*) Yeast cells coexpressed Uso1p-3xGFP (pNB1621) with GALpYpt1 (NY3210) or GALpYpt1SW1^{Sec4} (NY3211). (Scale bar, 5 μm.) (*D*) Quantification of cells exhibiting a polarized distribution of the indicated proteins. Error bars represent SD; $n = 3$.

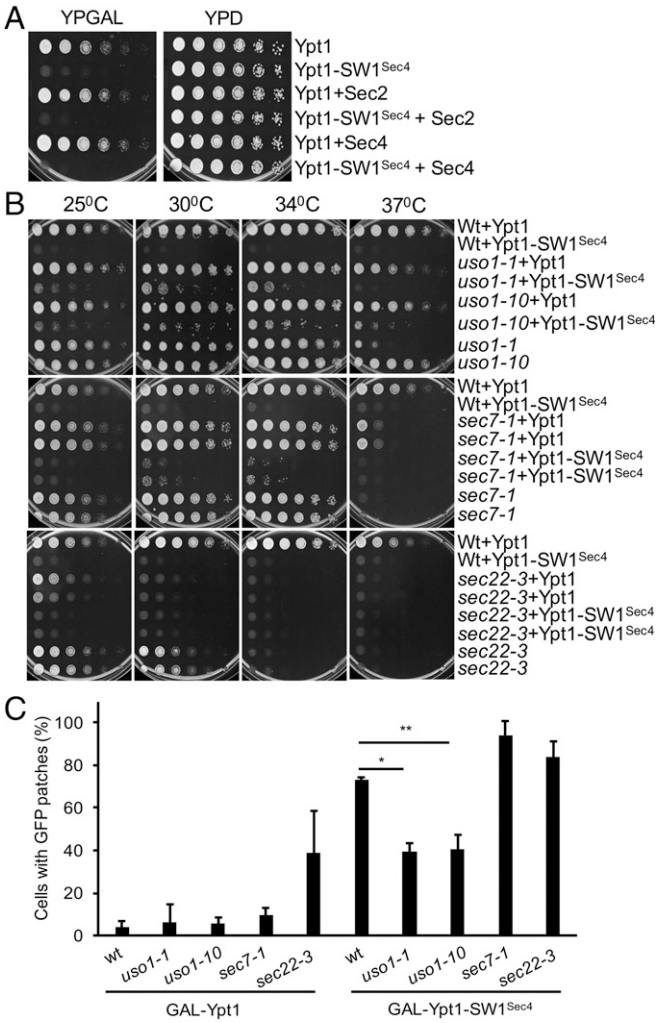

Fig. 7. The toxicity of high-level Ypt1-SW1^{Sec4} expression is suppressed by truncation of Uso1, but not by overexpression of Sec2 or Sec4. (*A*) Strains expressing GALpYpt1 (NY3196) or GALpYpt1-SW1^{Sec4} (NY3197) were transformed with a high copy-number plasmid carrying Sec2 (pNB134) generating strains NY3213 and NY3214 respectively or with a high copy-number plasmid carrying Sec4 (pNB1622), generating strains NY3215 and NY3216, respectively. Cells were grown to early stationary phase in selection medium, serially diluted, and spotted onto YPGAL or YPD plates, as indicated. Plates were incubated at 25 °C for 2 d. (*B*) Wild-type (NY3196, NY3197), *uso1-1* (NY3217, NY3218), *uso1-10* (NY3219, NY3220), *sec7-1* (NY3223, NY3224), and *sec22-3* (NY3225, NY3226) cells expressing Ypt1 or Ypt1-SW1^{Sec4} from the *GAL1* promoter were grown to early stationary phase in YPD medium at 25 °C, washed once, spotted onto YPGAL plates in fivefold serial dilutions, and then incubated at the indicated temperature for 3 d. Both *uso1* truncations, but neither *sec7-1* nor *sec22*-3, suppress the toxicity of Ypt1-SW1^{Sec4}. (*C*) Quantification of cells exhibiting an internal patch of GFP-Snc1 (see Fig. S4 for representative images). Error bars represent SD; $n = 3$. *$P < 0.00015$, **$P < 0.0011$.

1,123. This less-severe truncation does not cause growth defects; however, it too suppressed the galactose-dependent toxicity of GALp Ypt1-SW1^{Sec4} expression (Fig. 7*B*). As controls, we examined the effects of the *sec7-1* and *sec22-3* mutations on the galactose-dependent toxicity of GALp Ypt1-SW1^{Sec4} expression. Sec7 acts in the formation of secretory vesicles from the Golgi, while Sec22 is needed, like Uso1, for transport from the ER to the Golgi. The *sec7-1* mutation conferred only slight suppression of the galactose sensitivity, at 30 °C or 34 °C, while no suppression was seen by *sec22-3* at any temperature (Fig. 7*B*).

We next examined the effects of *uso1-10*, *sec7-1*, and *sec22-3* on GFP-Snc1 localization in cells expressing Ypt1-SW1^{Sec4} from the *GAL* promoter. Substantial suppression of the polarized GFP-Snc1 localization phenotype was observed in *uso1-1* and *uso1-10* cells. This was evident as a significant decrease in the number of cells exhibiting a polarized patch of GFP-Snc1 and a reappearance of GFP-Snc1 at the plasma membrane in some cells (Fig. 7*C* and Fig. S4). No suppression was observed in *sec7-1* or *sec22-3* cells (Fig. 7*C* and Fig. S4). We also confirmed partial suppression by *uso1-10* of the Bgl2 secretion defect of cells expressing Ypt1-SW1^{Sec4} from the GAL promoter (Fig. S5). The ability of *uso1* truncations to suppress the toxicity and transport defects resulting from GALp Ypt1-SW1^{Sec4} expression suggests that the recruitment of full-length Uso1 to the surface of secretory vesicles by Ypt1-SW1^{Sec4} blocks their ability to dock and fuse with the plasma membrane.

Uso1 is the yeast homolog of the mammalian p115 protein. Like p115, Uso1 has an amino-terminal globular head followed by a long, homo-dimeric, coiled-coil tail (42) (Fig. 8*A*). The head of p115 has been shown to bind Rab1 (43) and we find that the homologous region of Uso1 (amino acids 1–246) binds to Ypt1 (Fig. 8 *B* and *C*). The coiled-coil region of p115 includes a section that is SNARE-like in sequence. We found that the first half of the coiled-coil region of Uso1 (amino acids 726–1,246) binds to the syntaxin-related SNARE, Sed5 (Fig. 8*D*), but not to the other SNAREs involved in transport from the ER to the Golgi (Fig. S6 *B–D*). The globular head showed no affinity for Sed5 (Fig. S6*A*). The loss of the SNARE-like domain in *uso1-1* correlates with the acquisition of temperature-sensitive growth defects. The *uso1-10* allele includes both the globular head domain that binds to Ypt1, as well as the SNARE-like region implicated in binding to Sed5 and this allele confers normal growth. Because *uso1-10* suppresses the galactose-dependent toxicity of GALp Ypt1-SW1^{Sec4} yet confers no growth defect on its own, and the Uso1-10 protein still has the capacity to bind both of its ligands, Ypt1 and Sed5 in vitro, it is unlikely that suppression is the result of an upstream inhibition of the secretory pathway.

Discussion

Many Rabs are linked to adjacent Rabs through their GAPs and GEFs, forming regulatory circuits that are thought to trigger Rab transitions and thereby promote changes in the functional identity of the membrane as it flows along a transport pathway (1). We have probed the effect of rewiring one such regulatory circuit on the yeast secretory pathway. Early analysis of the Ypt1-SW1^{Sec4} chimera had indicated apparently normal Ypt1 function (27), yet the subsequent demonstration that Ypt1-SW1^{Sec4} could be activated efficiently by the Sec4 exchange factor, Sec2 (29), caused us to reexamine this situation. We considered the possibility that Sec2 might not actually activate Ypt1-SW1^{Sec4} in vivo as it does in vitro (29), however the suppression of a *bet3-1* mutation by Ypt1-SW1^{Sec4} expression as well as the colocalization of Ypt1-SW1^{Sec4} with Sec2 at sites of polarized exocytosis argues against this possibility.

Ectopic activation of Ypt1-SW1^{Sec4} on secretory vesicles by Sec2 would be expected to lead to a Rab "identity crisis," in apparent conflict with our earlier study showing little phenotypic effect (27). We now report that Ypt1-SW1^{Sec4} expression does indeed lead to trafficking defects, the severity of which correlates with the level of expression. Even normal expression of Ypt1-SW1^{Sec4}, which does not slow growth, causes a measurable inhibition of the final stage of the secretory pathway, after the Golgi-derived vesicles have been concentrated at polarized sites of exocytosis but before their fusion with the plasma membrane. Higher levels of expression potently block both secretion and cell growth. These results confirm the importance of Rabs to the identity of the membranes with which they are associated.

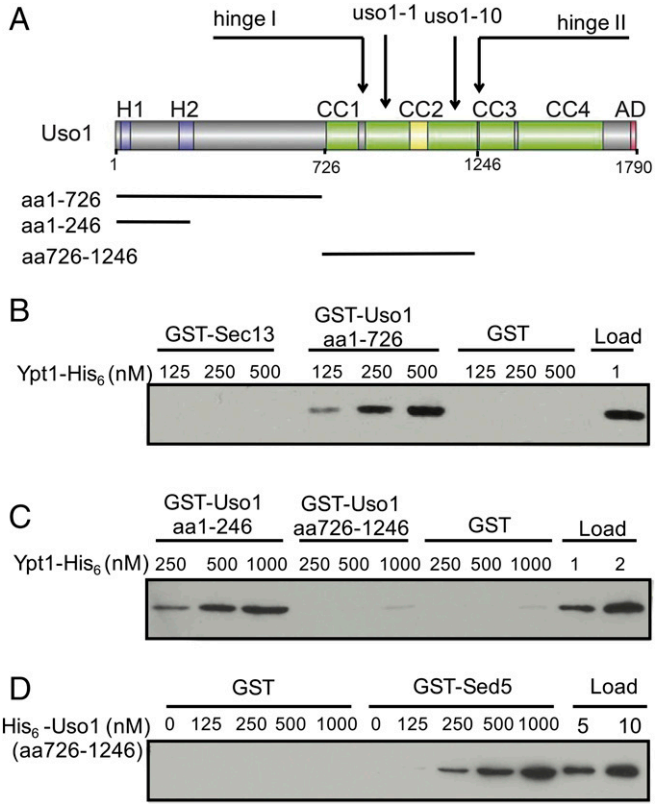

Fig. 8. Uso1 interacts with Ypt1 and Sed5. (*A*) A schematic diagram of the Uso1 protein. AD is an acidic domain; CC1–CC4 are coiled-coil regions; H1 and H2 are regions of homology between Uso1 and its mammalian homolog p115. A SNARE-like domain is highlighted in yellow within the CC2 region. The *uso1-1* mutation truncates the protein at aa 950, while *uso1-10* truncates the protein at amino acid 1,123. Hinge regions I and II were identified by Nakajima et al. (41). (*B* and *C*) The globular head domain of Uso1 interacts with Ypt1. GST-tagged Uso1 domains were immobilized on glutathione beads and then incubated with increasing amounts of purified His_6-Ypt1 proteins. GST and GST-Sec13 were used as controls. After washing, the bound His_6-Ypt1 was detected. (*D*) The CC1 and CC2 coiled-coil region of Uso1 (amino acids 726–1,246) binds to Sed5. GST-Sed5 was immobilized on glutathione beads and then incubated with increasing amounts of the His_6-Uso1 coiled-coil region (amino acids 726–1,246). After washing, the bound His_6-Uso1 was detected as described in *Materials and Methods*.

A key question is just how extensive is the reorganization of the secretory machinery in response to Ypt1-$SW1^{Sec4}$ expression. A literal interpretation of the Rab cascade model might predict that the entire Golgi would relocalize to polarized exocytic sites in response to Ypt1-$SW1^{Sec4}$ expression. The middle Rab on the pathway, Ypt32, did shift toward exocytic sites in agreement with the cascade model; however, of the three known Ypt1 effectors that we tested, only Uso1 exhibited a clear shift toward exocytic sites. While it is possible that the failure of the other two, Cog3 and Sec7, to relocalize could reflect a reduced affinity toward Ypt1-$SW1^{Sec4}$, the ability of *YPT1-SW1*^{Sec4} to replace *YPT1* argues against this interpretation. It appears more likely that Cog3 and Sec7 rely on additional interactions for their localization.

The observation that truncations of *uso1* suppress the toxicity and transport defects associated with Ypt1-$SW1^{Sec4}$ expression points to a probable mechanism of vesicular traffic inhibition. Uso1 forms a 155-nm-long homo-dimeric coiled-coil rod with a globular head at the amino terminal end (42). We show that the globular head binds to Ypt1 and the tail binds to the syntaxin-related Golgi tSNARE, Sed5. While truncation of the Uso1 rod before the Sed5 binding site (*uso1-1*) impairs ER–Golgi traffic (41), a less-severe truncation (*uso1-10*) does not; nonetheless, both truncations suppress Ypt1-$SW1^{Sec4}$ toxicity. Furthermore, neither the *sec22*-3 mutation, which inhibits ER–Golgi transport, nor the *sec7-1* mutation that blocks export from the Golgi, suppresses the toxicity. Thus, it is not the slowing of ER–Golgi traffic that leads to suppression. We propose that when Ypt1-$SW1^{Sec4}$ recruits full-length Uso1 by binding to its globular head, the long coiled-coil tail protrudes outward from the surface of secretory vesicles and sterically hinders their ability to dock and fuse with the plasma membrane. The truncations shorten the rod so that docking can proceed.

This model raises the interesting question of why Uso1 doesn't normally block the docking of ER-derived vesicles with the Golgi membrane by the same mechanism. The coiled-coil rod of Uso1 might bend to allow a closer approach of the vesicle to the Golgi. Rotary shadow EM revealed two hinge regions that correspond to breaks in the coiled-coil motif between residues 800–900 and 1,200–1,400 (42). This would be analogous to the related coiled-coil tethers EEA1 and the Golgin GCC185. In the case of EEA1, the rod collapses in response to binding Rab5-GTP (44), while in the case of GCC185, flexibility of a hinge region is essential for its function in endosome-Golgi traffic (45). It will be interesting to investigate if the conformation of Uso1 is regulated through its interaction with either Ypt1 or Sed5. Regulated bending could ensure that Uso1 not only promotes docking of vesicles to the correct target, but physically blocks docking to the wrong target. This would serve to increase the fidelity of vesicular traffic.

Materials and Methods

Yeast and Plasmid Strains Construction. The yeast strains and plasmids used in this study are listed in Tables S1–S3. To generate the various Ypt1-$SW1^{Sec4}$ expression plasmids, full-length Ypt1-$SW1^{Sec4}$ was PCR-amplified from NRB483 and inserted into the p416-GDP vector to generate (NRB1612) or into an integrative pRS306 based vector to generate NRB1615 at XbaI and XhoI sites. The plasmid was linearized with StuI and integrated into the yeast genome at the *URA3* locus. To generate GAL-inducible plasmids (NRB1617, NRB1619), the Ypt1-$SW1^{Sec4}$ PCR fragment was inserted behind the GAL1-10 promoter in pNB1383 or pNB1384 at BamHI/XbaI sites [NRB1383 pRS305 with Cyc1 term (SacII/SacI) + Adh term (ApaI/XhoI) + GAL1-10 promoter (SmaI/BamHI), and NRB1384 pRS306 with Cyc1 terminator (SacII/SacI) + Adh terminator (ApaI/XhoI) + GAL1-10 promoter (SmaI/BamHI)]. The plasmid expressing mCh-Ypt1-$SW1^{Sec4}$ (NRB1613) was generated by replacing the Ypt1 gene in pNR1326 with the Ypt1-$SW1^{Sec4}$ PCR fragment. This plasmid was linearized with AflII and integrated into the yeast genome at the *LEU2* locus. In each case, Ypt1 expression plasmids were generated in parallel to use as controls (NRB1611, NRB1614, NRB1616, NRB1618). Fusions of Uso1 or Cog3 protein to 3xGFP tags were constructed by PCR amplification of the C-terminal 1,000-bp fragment of *USO1* (NRB1621) or *COG3* (NRB1620) from wild-type yeast genomic DNA with SalI and BamHI sites, and cloned into the plasmid pPG5-3xGFP (NRB1302) (46) followed by linearization with ClaI or SpeI, accordingly, and transformed into yeast cells. All plasmids constructed in this study were verified by DNA sequencing. C-terminal truncations of Uso1 were constructed in SFNY 1841 as described in Longtine et al. (47). Truncations were confirmed by PCR analysis.

Growth Tests. Yeast cells were grown in yeast extract peptone dextrose (YPD) medium to stationary phase. Cells were washed once with sterile water and spotted on YPD plates in fivefold serial dilutions starting with an OD_{600} of 5. In the case of yeast strains harboring a CEN or 2-μm circle-based plasmid, cells were spotted on synthetic complete (SC) selection plates. Plates were left at the specified temperature for the indicated time. For GAL induction experiments, yeast cells were grown in YP medium containing 2% raffinose overnight and then spotted on YPGAL plates.

Fluorescence Microscopy and Quantitative Localization Analysis. Yeast strains harboring a GFP- or mCherry-tag were grown at 25 °C to early log phase (OD_{600} 0.4–0.6) in selective SC medium. Next, 500 μL of cells were pelleted and resuspended in growth medium. Fluorescence imaging was performed as described previously (48). In brief, images were acquired with a 100× oil-immersion objective lens (α Plan Apochromat 100×/1.46 oil DIC lens; Carl Zeiss) on a spinning disk confocal microscopy system (Yokogawa Electric Corporation), connected to a microscope (Observer Z1; Carl Zeiss) equipped with an electron multiplying charge-coupled device (CCD) camera (Cascasde II; Photometrics).

Excitation of GFP or mCherry was achieved using 488-nm argon and 568-nm argon/krypton lasers, respectively. For each sample, *z*-stacks with a 100- or 200-nm slice distance were generated. Images were analyzed using AxioVision software 4.8 (Carl Zeiss). For quantitation studies, three independent transformants were examined and at least 100 cells for each condition were scored. Three separate experiments were used to calculate the SD.

Invertase Secretion Assay. The invertase secretion assay was carried out as previously described by Shen et al. (48). Briefly, yeast cells were grown at 25 °C in YP or SC selection medium containing 5% glucose overnight to early log phase (0.3–0.5 OD/mL). Next, 1 OD_{600} unit of cells were transferred to two sets of 15-mL tubes, and pelleted. One set of cells were washed once with 0.5 mL sterile water and resuspended in 1 mL 10 mM NaN3, and kept on ice. This was for the 0-h samples. Another set of cells were washed once with sterile water, resuspended in 1 mL of YP or SC selection medium containing 0.1% glucose, and incubated at 37 °C with shaking for 1 h. Cells were pelleted and resuspended in 1 mL of 10 mM NaN_3. This set of cells was used for 1-h samples. For each 0- and 1-h sample, the external invertase was measured directly. The internal invertase was measured after 0.5 mL of cells were treated with 50 μg/mL zymolyase at 37 °C for 45 min to generate spheroplasts and lysed with 0.5 mL of 0.5% Triton X-100. The percentage of invertase secretion was calculated by [Ext (1 h) − Ext (0 h)]/{[Ext (1 h) − Ext (0 h)] + [Int (1 h) − Int (0 h)]} (18).

Bgl2 Secretion Assay. The Bgl2 secretion assay was performed as previously described (49). In brief, 50 mL of yeast cells were grown at 25 °C in YPD medium overnight to early log phase (~0.3 OD_{600}/mL). About 5 $OD_{600\ nm}$ units of cells were transferred to a sterile flask. Two sets of flasks were prepared for each strain. One set was incubated at 25 °C and the other set was at 37 °C. After 90-min incubation with shaking, both sets of cell cultures were harvested by centrifugation at 900 × *g* for 5 min. Cell pellets were resuspended in 1 mL of ice-cold 10 mM NaN_3 and 10 mM NaF, and then incubated on ice for 10-min. The suspension was transferred to microfuge tubes, pelleted, and resuspended in 1 mL of fresh prespheroplasting buffer (100 mM Tris·HCl, pH 9.4, 50 mM β-mercaptoethanol, 10 mM NaN_3, and 10 mM NaF), and incubated on ice 15-min. Cells were then pelleted and washed with 0.5 mL of spheroplast buffer (50 mM KH_2PO_4-KOH, pH 7.0, 1.4 M sorbitol, and 10 mM NaN_3), and resuspended in 1 mL of spheroplast buffer containing 167 μg/mL zymolyase 100T (Nacasai Tesque). Cells were incubated in a 37 °C water bath for 30 min. Spheroplasts were spun down at 5,000 × *g* for 10 min, and 100 μL of the supernatant from each tube was transferred into a new tube and mixed with 34 μL of 4× SDS sample buffer (the external pool). All of the remaining supernatant was discarded and the pellet (spheroplast) was resuspended in 100 μL 1× SDS sample buffer (the internal pool). Samples were loaded on a 10% SDS/PAGE gel. Bgl2 was visualized by Western blotting with anti-Bgl2 rabbit polyclonal antibody at 1:5,000 dilution (provided by the laboratory of Randy Schekman, University of California, Berkeley). As a loading control, Adh1 was visualized by Western blotting with anti-Adh1 rabbit polyclonal antibody (AB1202; EMD Millipore) at 1:10,000 dilution. For quantitation of Bgl2, samples used for immunoblotting were diluted accordingly to achieve approximately similar level of Bgl2 protein and loaded onto the same SDS/PAGE gel. Serial dilutions of a control sample were run in parallel to establish a standard curve. The electrophoretic bands were quantitated using ImageJ software (https://imagej.nih.gov).

Electron Microscopy. Yeast cells expressing Ypt1 (NY1048) or Ypt1SW1^{Sec4} (NY1052) at the normal level were grown at 25 °C in YPD to an $OD_{600\ nm}$ of ~0.5 and then processed for EM as previously described (50). In brief, ~10 $OD_{600\ nm}$ units of cells were collected using a 0.22-μm filter apparatus, washed with 10 mL of 0.1 M cacodylate (pH 6.8), then resuspended in 10 mL of fixative (0.1 M cacodylate, 4% glutaraldehyde, pH 6.8). Cells were fixed at room temperature for 1 h and then moved to 4 °C for 16 h. The next day, cells were washed twice with 50 mM KPi (pH 7.5), and then resuspended in 2 mL of 50 mM KPi buffer containing 0.25 mg/mL Zymolyase 100T. Cells were then incubated for 40 min at 37 °C in a water bath with gentle shaking. After the incubation, the cells were washed twice with ice-cold 0.1 M cacodylate buffer using a 0.22-μm filter apparatus, and resuspended in 1.5 mL of cold 2% OsO_4 in 0.1 M cacodylate buffer. Cells were then incubated for 1 h on ice, washed three times with water, and then incubated in 1.5 mL of 2% uranyl acetate at room temperature for 1 h. Cells were dehydrated by a series of ethanol washes and incubated overnight in Spurr resin. Cells were embedded in fresh Spurr resin and baked at 80 °C for at least 24 h. Sections were stained with lead citrate and uranyl acetate, and images were acquired using a transmission electron microscope (Tecnai G2 Spirit; FEI) equipped with a CCD camera (UltraScan 4000; Gatan). For yeast cells harboring a *GAL10* expression plasmid (NY3196, NY3197), cells were grown in a YP medium containing 2% raffinose overnight and then switched to a medium containing 2% galactose for 7 h at 25 °C and then processed for EM.

Immobilization of GST Fusion Proteins. For purification of GST fusion proteins, BL21(DE3) cells were incubated at 18 °C overnight with 0.5 mM isopropyl β-D-1-thiogalactopyranoside to induce protein expression. Cells were collected and resuspended in 1× PBS with 1 mM DTT and protease inhibitors. Cells were sonicated for 2 min total with 15-s on/off bursts on ice. Triton X-100 was added to a final concentration of 1% and lysates were incubated on ice for 15 min. Lysates were cleared through a 15-min centrifugation at 27,000 × *g*. The supernatant was incubated with 1 mL of 50% glutathione Sepharose beads (GE Healthcare) that had been prewashed with PBS for 1 h at 4 °C with rotation. The beads were washed extensively with PBS and stored at 4 °C.

Purification of His_6 Fusion Proteins. For purification of His_6-tagged fusion proteins, cells were incubated overnight at 18 °C with 0.5 mM isopropyl β-D-1-thiogalactopyranoside to induce protein expression. Cells were collected and resuspended in sonication buffer (20 mM Hepes pH 7.4, 150 mM NaCl, 1 mM DTT, 15 mM imidazole and protease inhibitors). Cells were sonicated for 2 min total with 15-s on/off bursts on ice. Lysates were cleared through a 15-min centrifugation at 27,000 × *g*. The supernatant was incubated with 2 mL of 50% Ni-NTA resin (Qiagen) for 1 h at 4 °C with rotation. The Ni-NTA resin was prewashed with sonication buffer. Following binding the resin was washed extensively with sonication buffer. Fusion proteins were eluted off the resin with sonication buffer with 250 mM Imidazole. Proteins were buffer exchanged with 20 mM Hepes (pH 7.4), 150 mM NaCl. Glycerol was added to a final concentration of 30% and proteins were stored at −20 °C.

In Vitro Bindings with Recombinant Proteins. Equimolar amounts (0.2 μM) of immobilized GST fusions were incubated with increasing amounts of bacterial purified His_6-Uso1 in binding buffer (25 mM Hepes pH 7.4, 150 mM NaCl, 2% Triton X-100, 1 mM $MgCl_2$, 1 mM EDTA, 1 mM DTT, protease inhibitors) for 4 h at 4 °C with rotation. Beads were washed three times with binding buffer and eluted in 25 μL of sample buffer by heating for 5 min at 100 °C. Binding studies with bacterially purified Ypt1-His_6 were performed as described above except with binding buffer II (25 mM Hepes pH 7.4, 150 mM NaCl, 0.5% Triton X-100, 1 mM $MgCl_2$, 1 mM EDTA, 1 mM DTT, protease inhibitors).

Bound proteins were resolved on SDS/PAGE gels and detected with mouse monoclonal anti-His.

ACKNOWLEDGMENTS. We thank Ms. Ying Jones from M. Farquhar's laboratory for preparation of samples for electron microscopy; Dr. Shuliang Chen for construcing strains of SFNY2447 and SFNY 2448; and Yejin Lee for preparing SDS-glycine gels. Anti-Bgl2 antibody was a generous gift from the laboratory of Dr. Randy Schekman (University of California, Berkeley). This study was supported by Grant GM82861 (to P.N.) and Grants GM114111 and GM115422 (to S.F.-N.) from the NIH.

1. Mizuno-Yamasaki E, Rivera-Molina F, Novick P (2012) GTPase networks in membrane traffic. *Annu Rev Biochem* 81:637–659.
2. Araki S, Kikuchi A, Hata Y, Isomura M, Takai Y (1990) Regulation of reversible binding of smg p25A, a ras p21-like GTP-binding protein, to synaptic plasma membranes and vesicles by its specific regulatory protein, GDP dissociation inhibitor. *J Biol Chem* 265:13007–13015.
3. Cabrera M, Ungermann C (2013) Guanine nucleotide exchange factors (GEFs) have a critical but not exclusive role in organelle localization of Rab GTPases. *J Biol Chem* 288:28704–28712.
4. Walch-Solimena C, Collins RN, Novick PJ (1997) Sec2p mediates nucleotide exchange on Sec4p and is involved in polarized delivery of post-Golgi vesicles. *J Cell Biol* 137:1495–1509.
5. Blümer J, et al. (2013) RabGEFs are a major determinant for specific Rab membrane targeting. *J Cell Biol* 200:287–300.
6. Grosshans BL, Ortiz D, Novick P (2006) Rabs and their effectors: Achieving specificity in membrane traffic. *Proc Natl Acad Sci USA* 103:11821–11827.
7. Bacon RA, Salminen A, Ruohola H, Novick P, Ferro-Novick S (1989) The GTP-binding protein Ypt1 is required for transport in vitro: The Golgi apparatus is defective in ypt1 mutants. *J Cell Biol* 109:1015–1022.
8. Jedd G, Richardson C, Litt R, Segev N (1995) The Ypt1 GTPase is essential for the first two steps of the yeast secretory pathway. *J Cell Biol* 131:583–590.
9. Benli M, Döring F, Robinson DG, Yang X, Gallwitz D (1996) Two GTPase isoforms, Ypt31p and Ypt32p, are essential for Golgi function in yeast. *EMBO J* 15: 6460–6475.
10. Jedd G, Mulholland J, Segev N (1997) Two new Ypt GTPases are required for exit from the yeast trans-Golgi compartment. *J Cell Biol* 137:563–580.

11. Salminen A, Novick PJ (1987) A ras-like protein is required for a post-Golgi event in yeast secretion. *Cell* 49:527–538.
12. Elkind NB, Walch-Solimena C, Novick PJ (2000) The role of the COOH terminus of Sec2p in the transport of post-Golgi vesicles. *J Cell Biol* 149:95–110.
13. Ortiz D, Novick PJ (2006) Ypt32p regulates the translocation of Chs3p from an internal pool to the plasma membrane. *Eur J Cell Biol* 85:107–116.
14. Mizuno-Yamasaki E, Medkova M, Coleman J, Novick P (2010) Phosphatidylinositol 4-phosphate controls both membrane recruitment and a regulatory switch of the Rab GEF Sec2p. *Dev Cell* 18:828–840.
15. Knödler A, et al. (2010) Coordination of Rab8 and Rab11 in primary ciliogenesis. *Proc Natl Acad Sci USA* 107:6346–6351.
16. Pusapati GV, Luchetti G, Pfeffer SR (2012) Ric1-Rgp1 complex is a guanine nucleotide exchange factor for the late Golgi Rab6A GTPase and an effector of the medial Golgi Rab33B GTPase. *J Biol Chem* 287:42129–42137.
17. Bustos MA, Lucchesi O, Ruete MC, Mayorga LS, Tomes CN (2012) Rab27 and Rab3 sequentially regulate human sperm dense-core granule exocytosis. *Proc Natl Acad Sci USA* 109:E2057–E2066.
18. Kinchen JM, Ravichandran KS (2010) Identification of two evolutionarily conserved genes regulating processing of engulfed apoptotic cells. *Nature* 464:778–782.
19. Nordmann M, et al. (2010) The Mon1-Ccz1 complex is the GEF of the late endosomal Rab7 homolog Ypt7. *Curr Biol* 20:1654–1659.
20. Wang F, et al. (2008) Varp interacts with Rab38 and functions as its potential effector. *Biochem Biophys Res Commun* 372:162–167.
21. Zhu H, Liang Z, Li G (2009) Rabex-5 is a Rab22 effector and mediates a Rab22-Rab5 signaling cascade in endocytosis. *Mol Biol Cell* 20:4720–4729.
22. Rana M, Lachmann J, Ungermann C (2015) Identification of a Rab GTPase-activating protein cascade that controls recycling of the Rab5 GTPase Vps21 from the vacuole. *Mol Biol Cell* 26:2535–2549.
23. Suda Y, Kurokawa K, Hirata R, Nakano A (2013) Rab GAP cascade regulates dynamics of Ypt6 in the Golgi traffic. *Proc Natl Acad Sci USA* 110:18976–18981.
24. Sasidharan N, et al. (2012) RAB-5 and RAB-10 cooperate to regulate neuropeptide release in *Caenorhabditis elegans*. *Proc Natl Acad Sci USA* 109:18944–18949.
25. Rivera-Molina FE, Novick PJ (2009) A Rab GAP cascade defines the boundary between two Rab GTPases on the secretory pathway. *Proc Natl Acad Sci USA* 106:14408–14413.
26. Du LL, Novick P (2001) Yeast rab GTPase-activating protein Gyp1p localizes to the Golgi apparatus and is a negative regulator of Ypt1p. *Mol Biol Cell* 12:1215–1226.
27. Brennwald P, Novick P (1993) Interactions of three domains distinguishing the Ras-related GTP-binding proteins Ypt1 and Sec4. *Nature* 362:560–563.
28. Dunn B, Stearns T, Botstein D (1993) Specificity domains distinguish the Ras-related GTPases Ypt1 and Sec4. *Nature* 362:563–565.
29. Dong G, Medkova M, Novick P, Reinisch KM (2007) A catalytic coiled coil: Structural insights into the activation of the Rab GTPase Sec4p by Sec2p. *Mol Cell* 25:455–462.
30. Cao X, Ballew N, Barlowe C (1998) Initial docking of ER-derived vesicles requires Uso1p and Ypt1p but is independent of SNARE proteins. *EMBO J* 17:2156–2165.
31. Cai Y, et al. (2008) The structural basis for activation of the Rab Ypt1p by the TRAPP membrane-tethering complexes. *Cell* 133:1202–1213.
32. Govindan B, Bowser R, Novick P (1995) The role of Myo2, a yeast class V myosin, in vesicular transport. *J Cell Biol* 128:1055–1068.
33. Donovan KW, Bretscher A (2015) Tracking individual secretory vesicles during exocytosis reveals an ordered and regulated process. *J Cell Biol* 210:181–189.
34. Novick P, Ferro S, Schekman R (1981) Order of events in the yeast secretory pathway. *Cell* 25:461–469.
35. Lewis MJ, Nichols BJ, Prescianotto-Baschong C, Riezman H, Pelham HR (2000) Specific retrieval of the exocytic SNARE Snc1p from early yeast endosomes. *Mol Biol Cell* 11: 23–38.
36. Novick P, Field C, Schekman R (1980) Identification of 23 complementation groups required for post-translational events in the yeast secretory pathway. *Cell* 21:205–215.
37. Harsay E, Bretscher A (1995) Parallel secretory pathways to the cell surface in yeast. *J Cell Biol* 131:297–310.
38. Harsay E, Schekman R (2002) A subset of yeast vacuolar protein sorting mutants is blocked in one branch of the exocytic pathway. *J Cell Biol* 156:271–285.
39. Suvorova ES, Duden R, Lupashin VV (2002) The Sec34/Sec35p complex, a Ypt1p effector required for retrograde intra-Golgi trafficking, interacts with Golgi SNAREs and COPI vesicle coat proteins. *J Cell Biol* 157:631–643.
40. McDonold CM, Fromme JC (2014) Four GTPases differentially regulate the Sec7 Arf-GEF to direct traffic at the trans-golgi network. *Dev Cell* 30:759–767.
41. Nakajima H, et al. (1991) A cytoskeleton-related gene, uso1, is required for intracellular protein transport in *Saccharomyces cerevisiae*. *J Cell Biol* 113:245–260.
42. Yamakawa H, Seog DH, Yoda K, Yamasaki M, Wakabayashi T (1996) Uso1 protein is a dimer with two globular heads and a long coiled-coil tail. *J Struct Biol* 116:356–365.
43. Allan BB, Moyer BD, Balch WE (2000) Rab1 recruitment of p115 into a cis-SNARE complex: Programming budding COPII vesicles for fusion. *Science* 289:444–448.
44. Murray DH, et al. (2016) An endosomal tether undergoes an entropic collapse to bring vesicles together. *Nature* 537:107–111.
45. Cheung PY, Limouse C, Mabuchi H, Pfeffer SR (2015) Protein flexibility is required for vesicle tethering at the Golgi. *eLife* 4:e12790.
46. Boyd C, Hughes T, Pypaert M, Novick P (2004) Vesicles carry most exocyst subunits to exocytic sites marked by the remaining two subunits, Sec3p and Exo70p. *J Cell Biol* 167:889–901.
47. Longtine MS, et al. (1998) Additional modules for versatile and economical PCR-based gene deletion and modification in *Saccharomyces cerevisiae*. *Yeast* 14:953–961.
48. Shen D, et al. (2013) The synaptobrevin homologue Snc2p recruits the exocyst to secretory vesicles by binding to Sec6p. *J Cell Biol* 202:509–526.
49. Liu D, Novick P (2014) Bem1p contributes to secretory pathway polarization through a direct interaction with Exo70p. *J Cell Biol* 207:59–72.
50. Chen S, Novick P, Ferro-Novick S (2012) ER network formation requires a balance of the dynamin-like GTPase Sey1p and the Lunapark family member Lnp1p. *Nat Cell Biol* 14:707–716.